

Non-destructive measurement of the dielectric constant of solid samples

A. Guadarrama-Santana and A. García-Valenzuela

*Centro de Ciencias Aplicadas y Desarrollo Tecnológico, Universidad Nacional Autónoma de México,
Apartado Postal 70-186 México D.F., 04510, México,*

e-mail: asur.guadarrama@ccadet.unam.mx; agosto.garcia@ccadet.unam.mx

Recibido el 18 de septiembre de 2009; aceptado el 1 de diciembre de 2009

We discuss and analyze a practical methodology for the determination of the dielectric constant of a macroscopic solid sample in a non-destructive way. The technique consists in measuring the capacitance between a pointer electrode and the dielectric surface as a function of the separation distance in a scale comparable to the radius of curvature of the tip's apex. The changes in capacitance that must be measured will commonly be in the atto-farad scale and require specialized instrumentation which we also describe here. The technique requires two calibration standards and the sample needs to have a portion of its surface flat and some minimum dimensions, but otherwise it can have an arbitrary shape. We used a simple model based on the method of images to explain the methodology and present experimental results with the proposed methodology.

Keywords: Capacitance measurements; dielectric constant; pointer electrode; materials characterization.

Se describe una metodología práctica para determinar la constante dieléctrica de una muestra sólida de una manera no destructiva. La técnica consiste en la medición de la capacitancia entre un apuntador y la superficie dieléctrica como función de la distancia de separación en una escala comparable al radio de curvatura de la punta. Los cambios en la capacitancia que se deben medir estarán normalmente en la escala de los ato-faradios y requieren de instrumentación especializada la cual también se describe aquí. La técnica requiere de dos patrones de calibración y la muestra necesita tener una porción plana en su superficie y con algunas dimensiones mínimas, pero fuera de eso puede tener una forma arbitraria. Utilizamos un modelo sencillo basado en el método de las imágenes para explicar la metodología y presentamos resultados experimentales con la metodología propuesta.

Descriptores: Mediciones capacitivas; constante dieléctrica; apuntador; caracterización de materiales.

PACS: 72.20.-I; 77.22.-d; 77.22.ch; 77.22.Ej; 77.22.Gm

1. Introduction

Capacitive measurements are commonly used to obtain the dielectric constant at low frequencies of liquids and solid films [1,2,3,4]. When determining the dielectric constant of solid samples by capacitance techniques, a sample with a specific shape and dimensions must be prepared. For instance, one may need to form a parallel plate capacitor with the sample for measurement [5]. In this respect capacitance techniques used with solid samples are destructive, since the sample must be cut and processed before measurement. The capacitive electrode geometry is very important because the capacitive value is directly in function of it. A few recent publications in this area have shown that capacitive measurements using spherical electrodes are more accurate [6]. However, the smaller the electrode's dimensions, the smaller the capacitance value one has to measure. It has been published that a thin tip electrode in close proximity to a surface can be used instead of a spherical electrode [2,7]. On the other hand, several groups have shown recently that it is possible to obtain capacitive measurement values in the order of atto-Farads with modern instrumentation. Nowadays, the surface capacitive image of thin film semiconductors is one application of interest where atto-Farad measurements are reported by several groups [8-11]. Also, in a recent publication we analyzed the capacitance of a spherical-electrode in contact with a dielectric-coating of finite thickness and found that the capacitance value is independent of the sample thickness

when the tip's radius is several times smaller than the sample's thickness [12].

In this work we show that it is possible to obtain the dielectric constant of a macroscopic solid sample in a non-destructive way and without knowing its precise dimensions by means of a metallic tip used as a capacitive electrode. Basically, the hypothesis of the methodology proposed here is that when using a pointer electrode with a sufficiently small radius at its apex in close proximity to the sample's surface, one can extract a contribution to the capacitance which is insensitive to the sample's dimensions but sensitive to the local relative permittivity of the dielectric sample. After a proper calibration procedure one can accurately measure the dielectric constant of solid samples with sufficiently large dimensions. The proposed methodology is non-destructive in the sense that it does not impose conditions on the general shape of the sample nor on the second capacitive electrode required to establish a potential difference.

The methodology proposed in this paper for extracting the tip's apex capacitance closely follows the one reported in Ref 2, developed for measuring the dielectric constant of very thin films. However, here we are interested in macroscopic solid samples with dimensions in the millimeter range and larger, so the model required here is different from that in Ref. 2. In the present methodology the apex capacitance variations are due to the electrical interaction between the tip's apex and the dielectric interface only, while the contri-

bution from the tip’s apex capacitance variations due to the interaction of the apex with the substrate are negligible. In fact, the capacitance variations measured here are neglected in the model used in Ref. 2. A calibration procedure for quantitative measurements of the dielectric constant is discussed in detail. Although, the capacitance variations that must be measured in the present application are in the attofarad range, as in capacitance microscopy and relate techniques, the requirements on the mechanical stage to handle the tip’s position are less demanding. We estimate the minimum ratio between the tip’s apex radius and the sample’s thickness to achieve a reasonable accuracy on determining the dielectric constant with the proposed methodology. On the other hand, the minimum apex radius will be determined by the minimum capacitance variation we can measure.

In Sec. 2 of this paper we describe the basic principles and assumptions of the proposed methodology. In Sec. 3 the measurement methodology and the experimental setup used in this work are described.

2. Principles of the proposed methodology

2.1. Basic principle

The basic idea behind the proposed methodology is relatively simple. Consider a flat interface between a medium of electric permittivity ϵ_x and a medium of electric permittivity ϵ_y . Suppose we place a conducting sphere of radius a in the first medium near the interface with the second medium. Using the method of images, it is not difficult to show that the capacitance is given by

$$C_s(s) = 4\pi\epsilon_1 a \sum_{i=0}^{\infty} \left\{ \prod_{j=1}^i \frac{a\Gamma}{2(a+s) - x_{j-1}} \right\}, \quad (1)$$

where s is the distance separating the sphere from the interface, $x = 0$,

$$x_n = \frac{a^2}{2(a+s) - x_{n-1}}, \quad \text{and} \quad \Gamma = \left(\frac{\epsilon_2 - \epsilon_1}{\epsilon_1 + \epsilon_2} \right).$$

Notice that when $i = 0$ in Eq. (1) we get 1 inside the curly brackets and thus the first term of the sum is $4\pi\epsilon_1 a$. Thus the capacitance of this ideal system is a function of the dielectric constants k_1 and k_2 of both media ($k_1 = \epsilon_1/\epsilon_0$ and $k_2 = \epsilon_2/\epsilon_0$, where ϵ_0 is the electric permittivity of vacuum) and of the radius of the spherical electrode, a . Clearly, if we know k_1 and a we may determine the dielectric constant k_2 from a measurement of the system’s capacitance at a known separation distance s . Due to random experimental errors in any measurement, it will be more accurate to retrieve the value of k_2 from a measured curve of the capacitance as a function of the distance s . In practice, due to parasitic capacitances in any real measurement, it will be necessary to measure capacitance differences. For instance, one could measure the difference in capacitance for two different values of s . In practice it will be convenient to choose one of the values of s to be zero.

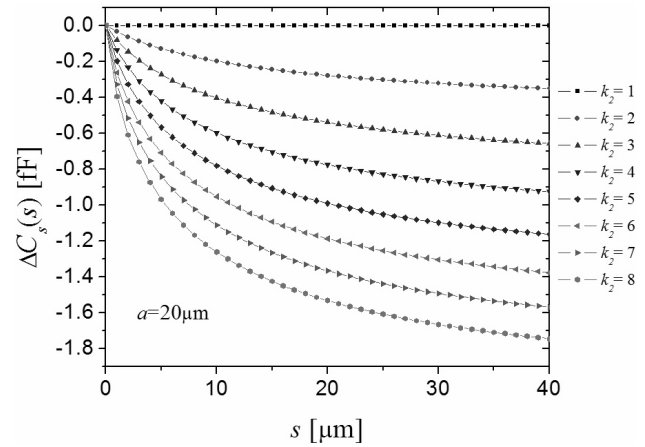


FIGURE 1. $\Delta C_s(s)$ curves for a sphere of radius $a=20\mu\text{m}$ and different values of the sample’s dielectric constant from $k_2=1$ to $k_2=8$. The curves were calculated with Eq. (1).

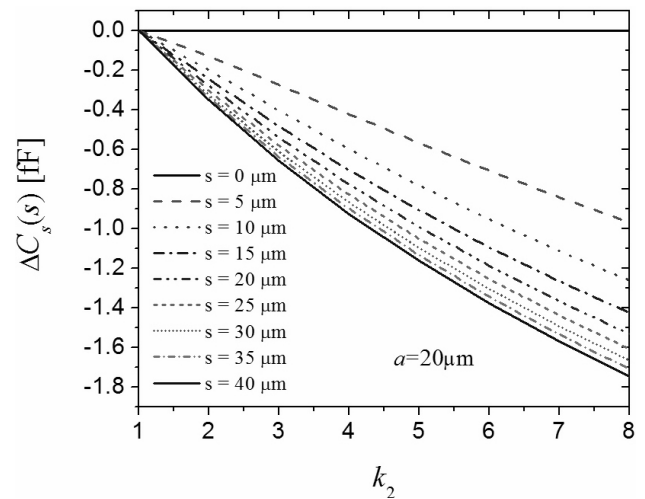


FIGURE 2. ΔC_s versus k_2 curves for a sphere of radius $a=20\mu\text{m}$ at different values of the separation distance s . The curves were obtained with Eq. (1).

In Fig. 1 we use Eq. (1) to plot $\Delta C_s(s) \equiv C_s(s) - C_s(0)$ versus s for a spherical electrode of $20\mu\text{m}$ radius in air ($k_1=1$) for several values of k_2 . In Fig. 2 we plot $\Delta C_s(s)$ for specific values of s as a function of k_2 for the same conducting sphere. The graphs in Figs. 1 and 2 suggest that using a $20\mu\text{m}$ spherical electrode and mechanical stage with micrometer resolution, it is possible to determine k_2 from the measurement of $\Delta C_s(s)$ in a scale of femto- to atto-farads.

In practice, however, the sample will not have infinite dimensions. To estimate when the dimensions of the sample are not large enough, let us consider the case of a dielectric film of finite thickness, d , as shown in Fig. 3. In this case, we may readily find a first correction to Eq. (1) using the method of images. Basically, we sum the first image charges on the conducting substrate arising from the image charges formed between the spherical electrode and the dielectric interface.

An exact solution to this problem would require one to continue this process and keep adding image charges of the image charges back and forth between the spherical electrode, the dielectric interface and the conducting substrate. However, here we only need an indication that the sample may not be considered of infinite dimension and thus we keep only the first set of image charges on the conducting substrate. In this case we get

$$C_f(s) = C_s(s) + 4\pi\epsilon_1 a \times \sum_{i=1}^{\infty} \left\{ \prod_{j=1}^i \frac{aM}{2(a+d+s) - y_{j-1}} \right\}, \quad (2)$$

where $y_0 = 0$, and

$$y_n = \frac{a^2}{2(a+d+s) - y_{n-1}} \quad \text{and}$$

$$M = \left(\frac{2\epsilon_1}{\epsilon_1 + \epsilon_2} \right) \left(\frac{2\epsilon_2}{\epsilon_1 + \epsilon_2} \right).$$

Notice that the sum in Eq. (2) starts for $i=1$, and thus the first term of the sum is $4\pi\epsilon_1 a^2 M / 2(a+d+s)$. Clearly, if $d \gg a$, then we have that $C_f(s) \rightarrow C_s(s)$. When the second term in Eq. (2) is not negligible, we may already suspect that the approximation of an infinite sample will not hold and the proposed methodology will incur in errors.

2.2. Obtaining the dielectric constant with a practical system

In practice we will not have an infinite surface nor an isolated sphere as an electrode. Instead, we will have a sample of finite dimensions and we could use a conducting pointer electrode attached to a cantilever in close proximity to the sample's surface as shown in Fig. 4. We will also have to use a second electrode beneath the sample to establish a potential difference between the conducting tip and the surface of the dielectric sample. The second electrode may be in simple contact with the sample. Of course, the capacitance of the system will be a complicated function of geometry of the electrodes, cantilever and sample. It will also have a parasitic

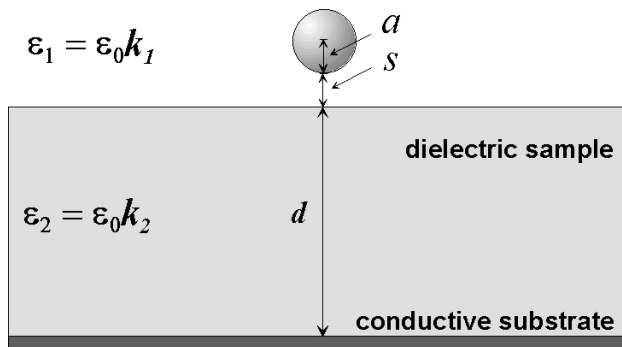


FIGURE 3. A spherical electrode on a dielectric film forming a capacitive system.

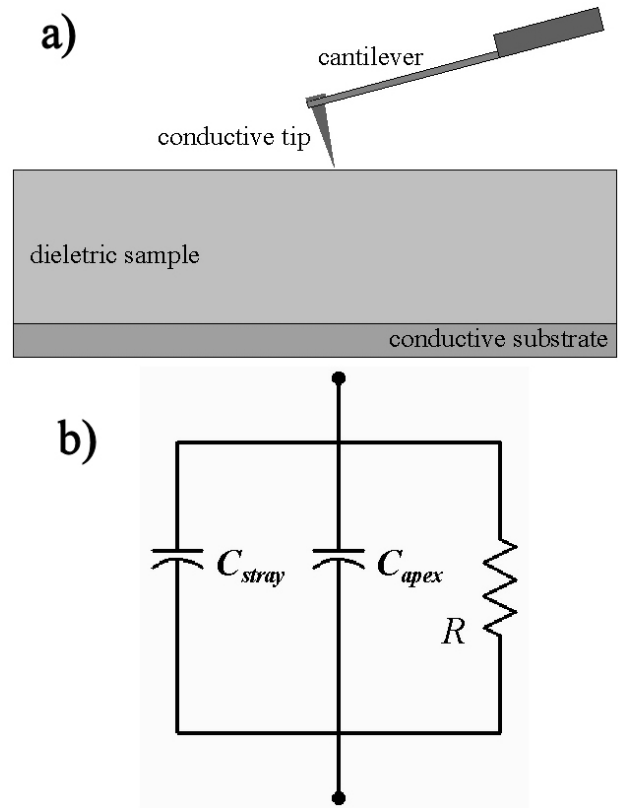


FIGURE 4. (a) Capacitive system with tip and cantilever used in practical measurements. (b) Equivalent RC circuit where C_{stray} represents the total stray capacitance produced by the tip cone, cantilever, chip, mechanical mounting and wiring and C_{apex} represents the apex-dielectric sample-substrate capacitance of interest and R is a finite resistance associated to the dielectric sample.

contribution from the electronics used. In general we can assume that the pointer will be in air and we may take, $k_1 = 1$, that is $\epsilon_1 = \epsilon_0$.

Nevertheless, if the radius at the apex of the pointer electrode is small compared to the dimensions of the sample and of the cantilever, we may separate the whole capacitance of the system in two: a contribution from the apex-surface region plus a contribution from the rest of the electrode, cantilever and electronics. Let us denote the contribution to the capacitance from the apex as C_{apex} and that due to the rest of the system as C_{stray} . Both C_{apex} and C_{stray} are functions of the tip-surface separation, s . Then we may write, $C(s) = C_{apex}(s) + C_{stray}(s)$. For $s \ll a$, where a is the apex's radius of curvature, $C_{stray}(s)$ will be a slowly varying function of s whereas $C_{apex}(s)$ will be a rapidly varying function. To some approximation, $C_{apex}(s)$ can be modeled as the capacitance of the isolated-sphere and infinite-surface given in Eq. (1). Since $C_{stray}(s)$ will be a slowly varying function of s , we may expand $C_{stray}(s)$ about $s = 0$ in a Taylor series and keep only the first two terms, that is, $C_{stray}(s) = C_{stray}(0) + \beta(k_2)s$, where $\beta(k_2) = [\partial C_{stray} / \partial s]_{s=0}$.

Experimentally, it is necessary to measure the capacitance change from a reference point. In practice, a convenient reference point is when the tip is in contact with the surface, that is, at $s = 0$. Then, let us define the “capacitance difference from contact” $\Delta C(s)$ as, $\Delta C(s) = C(s) - C(0)$. If the stray capacitance behaves linearly for not too large values of s , we have

$$\Delta C(s) = \Delta C_{apex}(s) + \beta(k_2)s, \quad (3)$$

where $\Delta C_{apex}(s) = C_{apex}(s) - C_{apex}(0)$. Now, Eq. (1) shows that $C_{apex}(s)$ tends rapidly to a constant value soon after s becomes larger than a . This means that in Eq. (3), $\Delta C(s)$ will tend to a linear function rapidly as s approaches the value of a and surpasses it.

Then we should measure $\Delta C(s)$ versus s from $s = 0$ until linear dependence with s is reached. We obtain the value of $\beta(k_2)$ and subtract the stray capacitance from Eq. (3) and obtain $\Delta C_{apex}(s)$ [2,7]. The function $\Delta C_{apex}(s)$ will depend on the dielectric constant of the sample, k_2 , and the apex’s dimensions only. In practice we may calibrate the system by obtaining $\Delta C_{apex}(s)$ for a few samples of known dielectric. Then we may define a convenient value of $s = s_m$ and adjust a curve $\Delta C_{apex}(s_m; k_2)$ that passes through the calibration points. If this curve is found to be smooth up to the maximum value of interest of k_2 , then two or three calibration points may suffice. To obtain the dielectric constant of a given sample in later measurements, we must measure ΔC_{apex} at $s = s_m$ and from the calibration curve we may retrieve the dielectric constant of the sample. In the rest of this paper we describe our experimental work showing the feasibility of the methodology.

3. Experimental work

3.1. Experimental considerations

When an ac voltage, $V_{ac}(\omega) = V_0 \exp(j\omega t)$, is applied between the tip and the substrate electrode, an ac current, $I_{ac}(\omega) = I_0 \exp(j\omega t)$, is established through the system. The capacitive system can be represented as an RC circuit in which a finite resistance R is in parallel with the capacitance of the tip’s apex with the sample’s surface, C_{apex} . As already mentioned, the tip is attached to a cantilever so that the tip’s cone, the cantilever, the whole mechanical structure and the wiring produce a stray capacitance C_{stray} also in parallel with the RC circuit as indicated in Fig. 4b.

An admittance analysis shows that

$$I_0 = (1/R + j\omega C_{apex} + j\omega C_{stray})V_0.$$

Thus the established current is out of phase with respect to the applied voltage and its imaginary part (*i.e.* the component 180° out of phase) is proportional to the capacitance of the system. We may then refer to the stray current $I_{stray} = j\omega C_{stray}V_0$, and the apex current, $I_{apex} = j\omega C_{apex}V_0$, both purely imaginary. Therefore, in

practice we can measure the capacitance by applying a voltage of constant amplitude at a fixed frequency and measuring the imaginary part of the current with a lock-in amplifier. The stray capacitance C_{stray} is typically orders of magnitude larger than C_{apex} and since any amplifier will have a finite dynamic range, it is necessary to subtract most of the current arising from the stray capacitance. Otherwise it would not be possible to resolve the small variations of C_{apex} . A technique to accomplish this was proposed and demonstrated by Lee, Pelz and Bhushan [10]. In order to reduce the stray current, the same voltage $V_{ac}(\omega)$ but shifted 180° in phase must be applied to a calibration capacitor with a capacitance C_{cal} close to C_{stray} at a reference position of the tip sample’s separation distance. The displacement current going through the calibration capacitor, $-I_{cal}$, and the current I_0 arrive at a common node and these two currents are added. The difference $I_0 - I_{cal} \equiv \Delta I$ must be in the order of magnitude of I_{apex} . After this node the contributions to the imaginary part of the current is the “apex” current, $I_{apex} = j\omega C_{apex}V_0$ plus the small difference current between the stray and calibration currents ΔI . The total current entering the Lock-in amplifier is $I_{Lock-in} = I_{dis} + I_{apex} + \Delta I$, where $I_{dis} = V_0/R$ is the dissipative current (real), as depicted in Fig. 5.

The capacitance value $\Delta C = C_{apex} + (C_{stray} - C_{cal})$ at a given separation distances is calculated with the following expression:

$$\Delta C = \frac{Im [I_{lock-in}(\omega)]}{\omega V_{ac}(\omega)}, \quad (4)$$

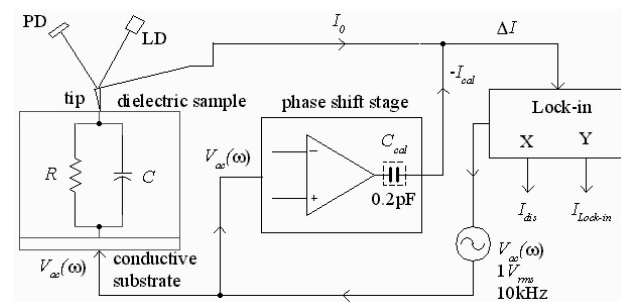


FIGURE 5. Block diagram of the capacitive measurement system in which the total current flow is shown. As can be seen, the current passes through the dielectric sample, tip, phase shift stage and finally to the lock-in amplification stage where the real and imaginary parts of the current are obtained.

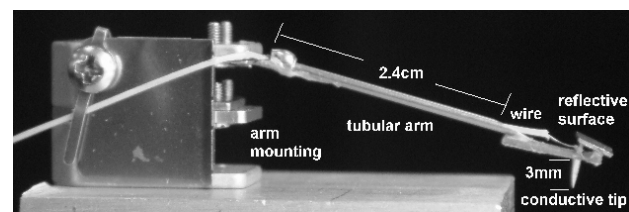


FIGURE 6. Complete tip and cantilever mounting with reflective surface on tip upper side, 3mm conductive tip and signal wire with tubular arm (guard).

where $I_{lock-in}(\omega)$ is the difference in currents at s and at $s = 0$, and $Im(\cdot)$ denotes the imaginary part. A fine-control of the current cancellation loop should be included so that $I_{apex} + \Delta I$ can be adjusted to zero at the reference separation distance $s = 0$.

3.2. Experimental setup

A 3 mm metallic tip was attached to a flexible cantilever 4 mm in length as shown in Fig. 4. The exact shape of the tip's apex could not be clearly observed under the microscope but an effective radius in the range of 20-40 μm was estimated. A reflective surface was mounted on the upper side of the cantilever in which a laser beam was reflected to a quadrant photo-detector in order to sense the tip tilt position, as it is shown in Fig. 6.

The cantilever with the tip was kept at a fixed height above a metallic sample holder mounted on a New Focus 8095 x, y, z mechanical-stage (positioner) with 16nm displacement per motor pulse approximately. The sample was placed on top of the sample holder and displaced upwards at 16 nm steps until the sample's surface made contact with the tip's apex. As soon as the tip makes contact with the dielectric sample's surface, the tip pushes the cantilever upwards and the reflected laser beam position on the quadrant photo-detector generates a signal indicating to stop the sample's displacement. The experimental setup is shown in Fig. 7.

Figure 7a shows the complete tip-sample mounting and Fig. 7b shows the laser beam and quadrant detector mounted to sense contact with the sample's surface. The whole system wiring was shielded and grounded before applying the voltage signal between the tip and metallic sample holder. The total capacitance of the experimental setup was around 0.2 pF. The total capacitance includes stray and apex-sample capacitances which were measured with a SR715 Stanford Research LCR meter with a 10 KHz frequency and 1 V_{rms} . We assembled a current cancellation circuit on a PCB (Printed Circuit Board) similar to that reported in Ref. [10]. The circuit consists of amplitude and phase shift stages. The ac voltage was compensated in amplitude and was 180° phase shifted. This voltage was applied to a calibration capacitor that was designed on the PCB.

Theoretically, the value of the calibration capacitor must be equal to the total capacitance of the experimental setup at some reference point. As already mentioned, the reference point is taken at $s = 0$, that is, when the tip is in contact with the sample's surface. The calibration capacitor was designed as a strip capacitor and was integrated in the PCB with the cancellation-current circuit as described in the Appendix. Once fabricated, the capacitance of the calibration capacitor was measured with the LCR meter and found to be $C_m = 0.205$ pF, close enough to the total capacitance of 0.2 pF. Since the calibration capacitor is fixed, to obtain a null current at the reference point $s = 0$ we adjusted as needed the amplitude and phase shift on the current passing through the calibration.

The methodology for measuring capacitance versus separation curves was the following. First, the dielectric sample was elevated until the tip's apex made "soft" contact with the dielectric sample upper surface. The current was then adjusted with the variable amplitude control to reach a sufficiently small value (typically ± 1 pico-ampere). The separation distance s was increased at fixed steps and the imaginary component of the current was registered with the Lock-in amplifier. Then $\Delta C(s)$ was calculated with Eq. (4) at each step of s . Later, the value of $\Delta C(0)$ was subtracted from all subsequent measurements of $\Delta C(s)$ and the curve of ΔC versus s was plotted. Also, a small offset on the experimental scale of the separations (smaller than one step) had to be subtracted to obtain a smooth and reproducible curve. The reason for this offset is that when the tip was brought into contact we could push the tip upwards, deflecting the cantilever a fraction of the last step. On the other hand, the mechanical stage presented a variable backlash depending on the size of the step chosen. In any case this offset was determined from the first few experimental points on a curve and subtracted.

3.3. Measurements

To calibrate our experimental setup we need three calibration points. Two of them may be obtained with two slabs of different materials of known relative permittivity, and an additional point may be obtained with air. (In this case one simply includes no sample in our setup.) The two calibration materials were chosen to be glass slab of the soda-lime type and a piece of PCB of the FR-4 type (according to the manufacturer) which is a hard dielectric material. To determine their relative permittivity, we deposited thin metallic films (by sputtering) on both sides of two calibration samples, forming a parallel plate capacitor with each of them. We measured the capacitance with the LCR meter and inverted the relative permittivity from the parallel-plate capacitor formula. We obtained a relative permittivity of 7.64 for the glass and of 4.87 for the FR-4 sample. Both slabs had a rectangular shape, 2 cm \times 2.5 cm. Due to edge effects we estimated that the latter values may be off from the real ones by at most 2% and a more rigorous procedure to generate calibration samples may be needed. However, we will ignore this possible error since it would only introduce a systematic error in future measurements of the dielectric constant with our experimental system, and here we are interested only in evaluating the feasible precision of the proposed methodology.

Measurements of $\Delta C(s)$ from $s = 0$ to $s = 40$ μm at steps of 1.6 μm were performed for two calibration slabs and for air. In the case of air, the reference point $s = 0$, was taken at a height of 1 mm from the metallic substrate. All current data were averaged within a 10 second time period with a 64 Hz sample rate and a 100 ms time constant with a standard deviation of $\sigma = \pm 1$ pA approximately. The current noise was $I_n = 0.91$ pA/ $\sqrt{\text{Hz}}$ with a noise equivalent bandwidth of 1.2 Hz (100 ms, 12 dB/oct time constant), and

$1V_{rms}$. Thus, we had an equivalent capacitance input noise of $C_n=14.5 \text{ aF}/\sqrt{\text{Hz}}$.

The experimental curves are plotted in Fig. 8. As can be seen the graphs, the curves change faster for values of s up to about $10 \mu\text{m}$ and tend to a straight line for larger values of s . The tangent lines to the end portions of the curves are also plotted in Fig. 8. The capacitance change due to the tip's apex is obtained by subtracting the asymptotic straight lines from the measured $\Delta C(s)$ curves as discussed above. The data for $\Delta C_{apex}(s)$ for air, FR-4 and glass are plotted in

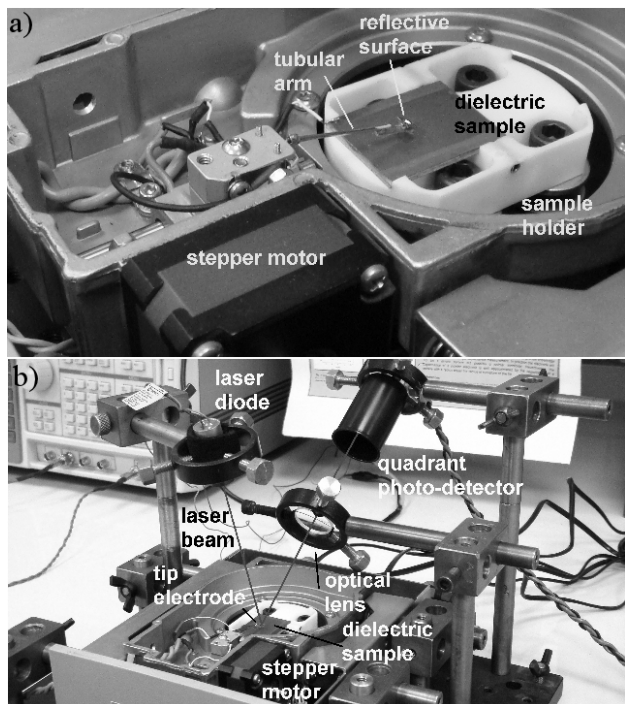


FIGURE 7. (a) Tip mounting, dielectric sample and sample holder over the nano-metric positioner. (b) Complete capacitive sensor mounting.

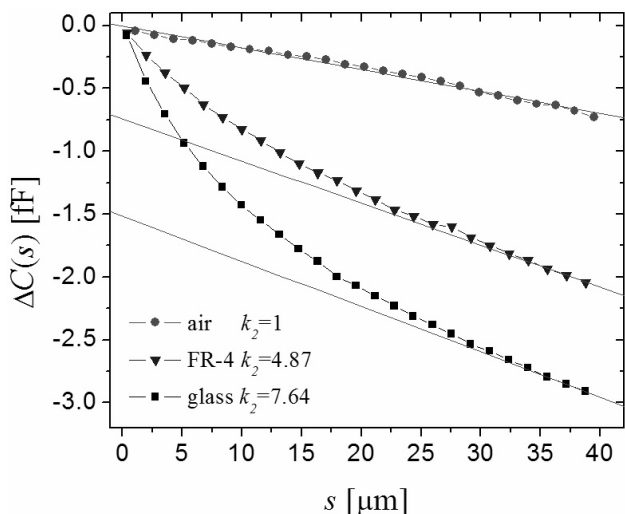


FIGURE 8. ΔC versus s experimental curves with offset correction and C_{stray} tangent lines.

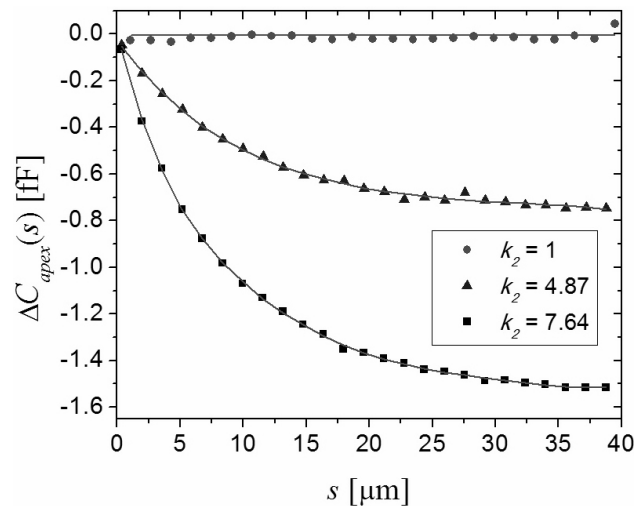


FIGURE 9. ΔC_{apex} versus s experimental fitted curves with linear, 5th and 7th orders for air, FR-4 and glass samples respectively with C_{stray} tangent lines subtracted.

Fig. 9. We also plot a fitted polynomial (linear, 5th and 7th order respectively) to each set of data. As can be seen in this figure, the three curves are well separated from each other.

Now, to obtain a calibration curve for future measurements of the dielectric constant of solid samples, we must choose a specific separation distance, s_m , and plot $\Delta C_{apex}(s_m)$ versus the relative permittivity k_2 . The specific value of s_m appears rather arbitrary. In Figs. 10a, 10b and 10c we plot $\Delta C_{apex}(s_m)$ versus k_2 for $s_m = 9 \mu\text{m}$, $17 \mu\text{m}$ and $33 \mu\text{m}$, respectively. In all cases a polynomial of second order fits the three calibration points very well. This shows that in our experimental setup we do not need more calibration points, and three is enough. In principle, with either of the three calibration curves we can measure the relative permittivity of a solid sample as long as this is near or smaller than that for the calibration glass.

Once we had the calibration curves for our setup, we continued to measure the relative permittivity of fused quartz. We measured $\Delta C(s)$ for a quartz slab about 1.7 mm thick for $s = 0$ to $s = 40 \mu\text{m}$ and using a 10 KHz signal. We subtracted the linear dependence as explained before and calculated $\Delta C_{apex}(s_m)$ for $s_m = 9 \mu\text{m}$, $17 \mu\text{m}$ and $33 \mu\text{m}$. These values are indicated in Figs. 10a, 10b and 10c, respectively. From the intersection point of the calibration curves with the corresponding value of $\Delta C_{apex}(s_m)$ we obtain a value for the relative permittivity of fused quartz at 10 KHz of 3.90, 3.92, and 3.88 for $s_m = 9, 17$ and $33 \mu\text{m}$, respectively. The difference between these values may be taken as a measure of the reproducibility error in determining the dielectric constant with our experimental setup. These values differ from each other by 1% or less, which is an acceptable error. We may also compare our measurements with the nominal value for the dielectric constant of 3.75 reported by the manufacturer of the quartz used. The difference is 5%. However the manufacturer does not specify the frequency at which the di-

electric constant is reported, which could explain the difference.

4. Discussion

We can observe that the curves for the sphere model given by Eq. (1) for a spherical and the experimental curves for ΔC_{apex} are alike. The shape and order of magnitude of the scales coincide and we may estimate an effective radius at the apex of the pointer electrode somewhat smaller than $20 \mu\text{m}$. Nevertheless, Eq. (1) cannot be fitted to all the data of ΔC_{apex} vs. s . On the one hand, the shape of the tip's apex may not be round with a constant radius of curvature. On the other hand, the spherical electrode model considers a complete sphere, whereas the apex of a conducting tip electrode may approximate a half-sphere. Therefore we should not expect Eq. (1) to fit all the experimental data well. However the sphere model does give us a clear indication as to the order of magnitude of the capacitance variations we need to measure.

As mentioned in Sec. 2, the shape of the sample may actually be arbitrary as long as it has a portion of its surface of sufficiently large dimensions flat and thick enough. The rest of the surface and volume of the sample, as well as the metallic sample-holder used as a second electrode, will contribute to stray capacitance, which is subtracted from the measurements.

The model of a uniform film of thickness d will not give us an accurate model for the stray capacitance. However, it can give us an estimation of the minimum dimensions of the flat area of the sample's surface and the minimum sample's thickness. In Fig. 11 we calculate the calibration curves $\Delta C(s_m)$ versus k_2 for $s_m = 15 \mu\text{m}$ and $a = 20 \mu\text{m}$ using Eq. (2) for dielectric films of decreasing thickness d . We can appreciate that the calibration curve remains nearly constant from $d = 1\text{mm}$ down to 0.1mm and it clearly moves away until $d = 0.05 \text{mm}$, that is $50 \mu\text{m}$. This result suggests that the dimensions of the sample must be only a few times larger than the sphere radius.

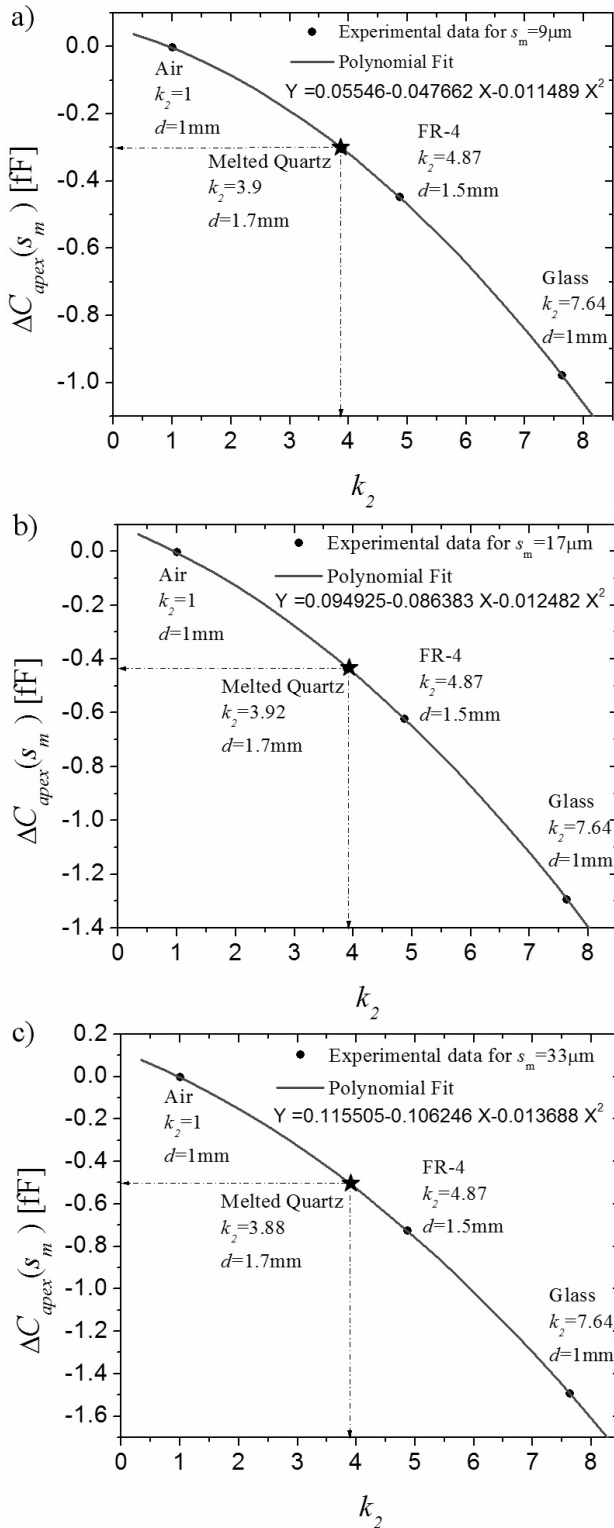


FIGURE 10. Relative permittivity of fused Quartz obtained with k_2 calibration curves for: a) $s_m=9\mu\text{m}$, b) $s_m=17\mu\text{m}$ and c) $s_m=33\mu\text{m}$.

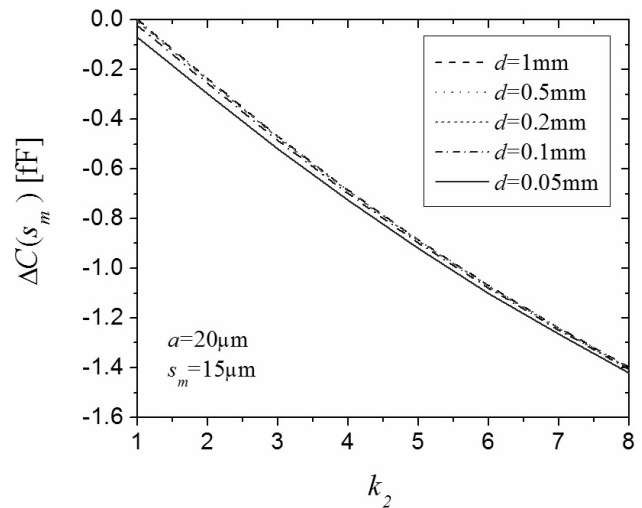


FIGURE 11. Calibration curves $\Delta C(s_m)$ vs. k_2 for $s_m = 15 \mu\text{m}$ and $a = 20 \mu\text{m}$ obtained with Eq. (2).

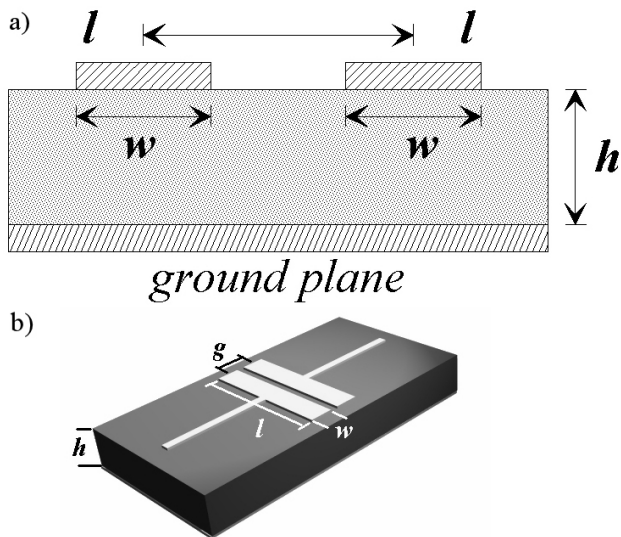


FIGURE 12. (a) Scheme of the parallel strips with a conductive grounded plane in a PCB. (b) Complete scheme of the calibration capacitor.

It is not difficult to show that if the dimensions of a 3D problem are scaled by a factor p while keeping the same relative electric permittivity, then the capacitance is scaled by the same factor p . In the methodology proposed in this paper, the scale is dictated by the radius at the tip's apex. The methodology could be used at smaller scales provided one is able to measure smaller variations of the capacitance. In our experimental measurements we had a standard deviation of $\sigma = \pm 1\text{pA}$ approximately which give us an uncertainty in measuring capacitance variations of about 16 aF. If the uncertainty on capacitance variations is improved to 1 aF, we could reduce the tip's apex radius 16 times to about 1 or 2 μm without losing resolution on the measurement of the dielectric constant. The methodology may also be used at larger scales and in this case the required instrumentation may be somewhat simpler.

The resolution of the mechanical stage required to vary the separation between the sample and the tip will depend on the scale. In our experimental setup, the effective tip's apex radius was about 20 μm and the step in changing s was 1.6 μm . We could have used a simpler mechanical stage and the step could have been somewhat larger. In any case, if the tip's radius is increased or decreased the step in s may be increased, or decreased accordingly.

5. Conclusions

We presented a new methodology to measure the relative electric permittivity of solid samples. This methodology may be used in a non-destructive way in many cases for samples of different shapes. It is not necessary to deposit thin metallic films on the sample to perform as electrodes. The sample does not need to be cut into a particular shape or size, but a flat area of the sample's surface of some minimum dimensions as well as a minimum thickness is needed. Basically,

the technique requires a capacitance meter, a metallic tip with the appropriate apex's radius, a mechanical stage, and two calibration standards. Although our experimental setup can be improved in several respects, we believe that the results presented here prove the feasibility of the proposed methodology and shows that a resolution on the determination of the dielectric constant below 1% is possible.

Acknowledgements

We are grateful to Alejandro Esparza for his technical assistance in thick film deposit on dielectric samples, Blas Sánchez for his technical assistance in sample holder fabrication and to the Dirección General de Asuntos del Personal Académico and Dirección General de Estudios de Posgrado from the Universidad Nacional Autónoma de México for financial support during the realization of this work.

Appendix

The value of the calibration capacitor must be as near as possible to the total stray capacitance $C_{stray} = 0.2$ pF of the experimental setup. In addition, a fine control is needed in order to achieve a zero calibration before performing current measurements to determine values of ΔC .

The calibration capacitor was designed to be integrated into the PCB design of the phase shift stage in order to avoid external wiring and therefore, an increment of the stray capacitance.

The calibration capacitor design was based in mutual capacitance calculus between conductive strips separated from a conductive grounded plane by means of a dielectric film. The mutual capacitance C_m is a function of the spacing between strips (g), strip length (l), strip width (w), FR-4 relative permittivity (ϵ_r) and FR-4 thickness (h) as depicted in Fig. 12a. An additional contribution to the capacitance arises from the narrow strips connecting the capacitor to the rest of the circuit (see Fig. 12b).

A first approximation to the dimensions of the strip capacitors was obtained using the formula [13],

$$\frac{C_m}{l} = \frac{\epsilon p_1 p_2 \ln \left[1 + \left(\frac{2h}{g} \right)^2 \right]}{(4\pi \frac{h}{w})} \quad (\text{A.1})$$

where

$$p_1 = (716) \left(\frac{2h}{w} \right) + 1 \quad \text{and}$$

$$k_2 \approx 0.66 \left(\frac{2h}{w} \right) + 1.55.$$

Then with finite element numerical calculations and taking into account the narrow strips feeding the capacitor we adjusted the final dimensions of the parallel strips and spacing g between them to make of C_m approach the value of

C_{stray} . The final dimensions were $l = 1.6$ cm, $w = 3$ mm and $g = 0.8$ mm. We fabricated the printed capacitor on the PCB

and measured its capacitance SR715 Stanford Research LCR meter. We obtained $C_m = 0.205$ pF at 10 KHz frequency.

-
1. Hongshen Ma, J.H. Lang, and Alexander H.Slocum, *Review of Scientific Instruments* **79** (2008) 035105.
 2. L. Fumagalli, G. Ferrari, M. Samprieto, and G. Gomila, *Applied Physics Letters* **91** (2007) 243110.
 3. Jiaping Wu and J.P.W. Stark, *Meas. Sci. Technol.* **17** (2006) 781.
 4. A.P. Gregory and R.N. Clarke, *Meas. Sci. Technol.* **16** (2005) 1506.
 5. C. Cooke and J.E. Ford, *J. Phys. E: Sci. Instrum* **14** (1981).
 6. Ren-jie Zhang, Shu-guang Dai, and Ping-an Mu, *Meas. Sci. Technol* **8** (1997) 1028.
 7. Kazuya Goto and Kazuhiro Hane, *Journal of Applied Physics*, **84** (1998) 4043.
 8. L. Fumagalli, G. Ferrari, M. Samprieto, and G. Gomila, *Nano Letters* **9** (2009) 1604.
 9. L. Fumagalli *et al.*, *Nanotechnology* **17**(2006) 4581.
 10. D.T. Lee, J.P. Pelz, and Bharat Bhushan, *Review of Scientific Instruments* **73** (2002) 3525.
 11. S. Lányi, *Surface and Interface Analysis* **27** (1999) 348.
 12. A. Guadarrama-Santana and A. García-Valenzulela, *Key Engineering Materials* **381** (2008) 533.
 13. R.P. Arney, *Sensores y Acondicionadores de Señal*, 3ª edición, (Alfa mega grupo editor, S.A. de C.V 2001) p. 155.